Neurobiology of Disease 73 (2015) 388–398

Contents lists available at ScienceDirect

Neurobiology of Disease

journal homepage: www.elsevier.com/locate/ynbdi

Characterisation of immune cell function in fragment and full-length Huntington's disease mouse models

Ulrike Träger [a,1], Ralph Andre [a,1], Anna Magnusson-Lind [a,b], James R.C. Miller [a], Colúm Connolly [c], Andreas Weiss [d,2], Stephan Grueninger [d], Edina Silajdžić [b], Donna L. Smith [e], Blair R. Leavitt [c], Gillian P. Bates [e], Maria Björkqvist [b], Sarah J. Tabrizi [a,*]

[a] UCL Institute of Neurology, Dept. of Neurodegenerative Disease, London, UK
[b] Wallenberg Neuroscience Centre, Dept. of Experimental Medical Science, Brain Disease Biomarker Unit, Lund University, Lund, Sweden
[c] Centre for Molecular Medicine and Therapeutics, Department of Medical Genetics, University of British Columbia, Vancouver, BC, Canada
[d] Novartis Institutes for BioMedical Research, Novartis Campus, Basel, Switzerland
[e] King's College London, Dept. of Medical and Molecular Genetics, Guy's Hospital, London, UK

ARTICLE INFO

Article history:
Received 5 February 2014
Revised 30 September 2014
Accepted 20 October 2014
Available online 29 October 2014

Keywords:
Huntington's disease
Neurodegeneration
Neuroinflammation
Innate immune system
Myeloid cells
Cytokines
Animal models of disease

ABSTRACT

Inflammation is a growing area of research in neurodegeneration. In Huntington's disease (HD), a fatal inherited neurodegenerative disease caused by a CAG-repeat expansion in the gene encoding huntingtin, patients have increased plasma levels of inflammatory cytokines and circulating monocytes that are hyper-responsive to immune stimuli. Several mouse models of HD also show elevated plasma levels of inflammatory cytokines. To further determine the degree to which these models recapitulate observations in HD patients, we evaluated various myeloid cell populations from different HD mouse models to determine whether they are similarly hyper-responsive, as well as measuring other aspects of myeloid cell function. Myeloid cells from each of the three mouse models studied, R6/2, *Hdh*Q150 knock-in and YAC128, showed increased cytokine production when stimulated. However, bone marrow CD11b^{+} cells did not show the same hyper-responsive phenotype as spleen and blood cells. Furthermore, macrophages isolated from R6/2 mice show increased levels of phagocytosis, similar to findings in HD patients. Taken together, these results show significant promise for these mouse models to be used to study targeting innate immune pathways identified in human cells, thereby helping to understand the role the peripheral immune system plays in HD progression.

Huntington's disease (HD) is an autosomal dominant inherited neurodegenerative disease caused by a CAG-expansion in exon 1 of the huntingtin (*HTT*) gene, resulting in a mutant form of the protein (mHTT) that contains an elongated polyglutamine tract (The Huntington's Disease Collaborative Research Group, 1993). It is characterised by motor, cognitive and neuropsychiatric symptoms, which are associated with a loss of medium spiny neurons in the striatum and other changes in the CNS (Vonsattel and DiFiglia, 1998). However, patients are also affected by peripheral symptoms such as weight loss, muscle wasting and inflammation (van der Burg et al., 2009).

Animal models are a vital tool to research genetic diseases. In HD, many animal models have been established, including invertebrate models such as *Drosophila melanogaster* (Kazemi-Esfarjani and Benzer, 2000) and *Caenorhabditis elegans* (Parker et al., 2001), and mammalian models from rodents (Crook and Houseman, 2011) to primates (Yang et al., 2008). Invertebrate models have great potential for drug discovery studies such as therapeutic screens due to their short life-span and cost efficiency (Voisine et al., 2007), but they may not always be useful due to their relative lack of homology to the human genome. For example, invertebrate immune responses are very different to those in humans, with an innate immune system that shows distinct differences and the complete absence of an adaptive immune system (Beck and Habicht, 1996).

A variety of HD mouse models have been developed. The most widely used and best characterised is the R6/2, which ubiquitously expresses the 5′ end of the human *HTT* gene carrying only exon 1 with 150 CAG repeats (Mangiarini et al., 1996). The mice demonstrate a fast and progressive phenotype with a very early symptomatic onset at 6–8 weeks, showing motor symptoms, loss of brain volume and peripheral changes such as weight loss (Bjorkqvist et al., 2006; Li et al., 2005; Mangiarini et al., 1996). Moreover, these mice are a model of the mis-splicing of the *HTT* gene that occurs to generate an exon 1 HTT protein in all full length HD mouse models (Sathasivam et al., 2013).

* Corresponding author at: Department of Neurodegenerative Disease, UCL Institute of Neurology, Queen Square, London WC1N 3BG, UK. Fax: +44 207 676 2180.
E-mail address: s.tabrizi@ucl.ac.uk (S.J. Tabrizi).
Available online on ScienceDirect (www.sciencedirect.com).
[1] These authors contributed equally.
[2] Present address: IRBM Promidis, Pomezia, Italy.

http://dx.doi.org/10.1016/j.nbd.2014.10.012

Transgenic and knock-in mouse models expressing full-length mHTT have also been developed. The *Hdh*Q150 model was generated by knocking-in an expanded repeat of 150 CAGs into the mouse *Htt* gene (Lin et al., 2001) and develops progressive HD related phenotypes until end-stage disease at approximately 22 months of age (Woodman et al., 2007). At late-stage disease, the R6/2 mice (12–14 weeks) are remarkably comparable to *Hdh*Q150 mice (22 months), with both models exhibiting weight loss, motor abnormalities and widespread mHTT aggregates throughout the brain (Woodman et al., 2007), aggregates in peripheral tissues (Moffitt et al., 2009), highly comparable transcriptional profiles (Kuhn et al., 2007) and a progressively impaired heat shock response (Labbadia et al., 2011). YAC128 mice are transgenic for the full-length human *HTT* gene originally containing 128 CAG repeats (Slow et al., 2003). They develop progressive motor deficits from the age of six months, and show selective cortical and striatal atrophy at nine months (Van Raamsdonk et al., 2005).

HD patients have elevated plasma levels of inflammatory cytokines and chemokines (Bjorkqvist et al., 2008; Wild et al., 2011), and their monocytes are hyper-reactive following lipopolysaccharides (LPS) stimulation in vitro (Träger et al., 2014). In mice, the R6/2, *Hdh*Q150 and YAC128 models each have similarly elevated plasma levels of inflammatory cytokines (Bjorkqvist et al., 2008). Myeloid cells from both R6/2 and BACHD mice have also been shown to migrate abnormally (Kwan et al., 2012b), demonstrating that they are affected by mHTT expression. Here, myeloid cells from different HD mouse models were evaluated to assess whether they are similarly hyper-responsive, like HD patient cells. We analysed cytokine production and other key immune cell functions in cultured cells, comparing several commonly-studied myeloid cell populations from blood, spleen and bone marrow.

Materials and methods

Animals

Mice from colonies at King's College London (KCL) were used for the cytokine profiling, phagocytosis assays and FACS analyses. R6/2 mice (Mangiarini et al., 1996) were bred by backcrossing hemizygous males to (CBA × C57BL/6)-F1 females (B6CBAF1/OlaHsd; Harlan, UK). *Hdh*Q150 homozygous mice on a (CBA × C57BL/6) F1 background ($Hdh^{150Q/150Q}$) were obtained by inter-crossing *Hdh*Q150 heterozygous CBA/Ca and C57BL/6J congenic lines as described previously (Woodman et al., 2007). For the differentiation and cell adhesion assays, R6/2 mice from a colony at Lund University were used (Jackson Laboratories, USA), obtained by crossing heterozygous (C57BL/6) males with (C57BL/6) females. Experiments using YAC128 mice were undertaken at the University of British Columbia, Vancouver. All animals had unlimited access to food and water, were subject to a 12-h light/dark cycle and housing conditions and environmental enrichment were as previously described (Hockly et al., 2003).

At KCL, R6/2 and *Hdh*Q150 mice were genotyped by PCR using genomic DNA isolated from an ear-punch and the *Htt* CAG repeat length was measured as previously described (Sathasivam et al., 2010). The CAG repeat size for the KCL R6/2 mice was 209.3 ± 8.5 and for the *Hdh*Q150 mice it was 163.3 ± 2.8. At Lund University, tail tips were taken at 4 weeks of age and genotyped by PCR at Laragen (Laragen, USA). The CAG repeat length size for the Lund R6/2 mice was 240–252 repeats. The YAC128 mice had a CAG repeat length of 120 ± 0.343.

At KCL, all experimental procedures were approved by the Local Ethics Committee and performed under a project licence issued by the UK Home Office. Experimental procedures at Lund University were carried out in strict accordance with Swedish legislation and approved by the Animal Ethics Committee in Lund and Malmö, Sweden, and at the University of British Columbia they were performed in accordance with protocols approved by the University of British Columbia Committee on Animal Care and the Canadian Council on Animal Care.

Isolation of primary murine cells

Blood monocytes

Blood was obtained by cardiac puncture, collected into EDTA coated tubes (BD Vacutainer), and 1 ml red blood cell lysis buffer (ammonium chloride buffer; eBioscience) was added per 1 ml of blood. The samples were then incubated for 5 min at room temperature. Following centrifugation at 300 ×*g* for 5 min, the lysis step was repeated twice. Cells were then resuspended in 270 μl MACS buffer (PBS including 1% bovine serum albumin (BSA) and 2 mM EDTA) and 30 μl anti-mouse CD11b magnetic beads. After 15 min incubation in the fridge, the samples were washed in MACS buffer (300 ×*g* for 5 min), resuspended in 500 μl MACS buffer and loaded on pre-wetted MACS columns placed in the magnet. After allowing the cell suspension to flow through by gravity, the columns were washed three times with 1 ml MACS buffer. Labelled $CD11b^+$ monocytes were eluted by removing the columns from the magnetic field.

Bone marrow

Mice were sacrificed by neck dislocation or by rising concentration of CO_2. Femur and tibia were dissected at the hip joint and any remaining muscle tissue was carefully removed. The bones were placed in a petri dish filled with cold RPMI-1640 media and cut at the joints. Bone marrow was flushed out by rinsing the shaft with media using a 5 ml syringe and 26 gauge needle. Lumps of cells were disaggregated by pipetting up and down several times before the cells were passed through a 70 μm nylon cell strainer. After washing with RPMI-1640 media (centrifugation at 300 ×*g* for 5 min) cells were counted using a Neubauer counting chamber. The cell suspension was labelled with 10 μl anti-mouse CD11b magnetic beads and 90 μl MACS buffer per 1×10^7 cells, and sorted as described above. When seeded in culture the isolated CD11b positive cell population resembled an early monocyte population, which could then be differentiated into bone marrow-derived macrophages. For the differentiation, sorted bone marrow cells were cultured in R10 media (RPMI-1640 supplemented with 10% FBS, 2 mM L-glutamine, 50 units/ml penicillin and 50 mg/ml streptomycin supplemented with 20 ng/ml recombinant murine M-CSF). After 3 days cells were provided with fresh media and growth factor. The cells resembled a macrophage phenotype from day 6.

Spleen

Spleens were dissected from the mice and stored in RPMI-1640 media until the preparation was started. To obtain a single cell suspension, spleens were cut into pieces and digested using 2 ml digestion buffer (RPMI-1640 media including 10% FBS, 15 mM HEPES, 0.5% collagenase type 4 (C1889; Sigma-Aldrich)). After 30 min incubation at room temperature the remaining spleen pieces were filtered through a 70 μm nylon cell strainer (BD Falcon). Afterwards, the splenocytes were centrifuged (300 ×*g* for 5 min) and the pellet was incubated with 1 ml red blood cell lysis buffer for 5 min at room temperature. Cells were then counted using a Neubauer counting chamber and isolated using 10 μl anti-mouse CD11b magnetic beads and 90 μl MACS buffer per 1×10^7 cells as described for blood monocytes.

Peritoneal macrophages

In order to prevent bleeding into the abdominal cavity, mice were killed using a rising concentration of CO_2. Fur covering the peritoneum was carefully removed and 5 ml of ice-cold, serum free RPMI1640 medium was injected into the abdominal cavity using a 26 gauge needle. After massaging the mouse abdomen for 1–2 min, cells were recovered through a small incision using a sterile plastic Pasteur pipette and put on ice as quickly as possible. The centrifuged (5 min at 300 ×*g*) cell suspension was incubated with 1 ml red blood cell lysis for 5 min at room temperature. Afterwards, the cells were washed with PBS (centrifuged at 300 ×*g* for 5 min). The resultant cell suspension contained macrophages as well as neutrophil, so cultures were enriched for

macrophages by removing non-adherent neutrophils by media changing and washing the cells after 2 h in a culture.

Cytokine profiling of R6/2 and HdhQ150mice

Blood monocytes isolated from *HdhQ150* mice were seeded at 100,000 cells into 96-well plates in 100 μl R10 media. Due to low yields from R6/2 mice, cells were pooled according to genotype and multiple wells were seeded at 100,000 cells into 96-well plates in 100 μl R10 media. Splenic and bone marrow monocytes were seeded in 24-well plates at a density of 500,000 cells per well. All cultures were primed with 10 ng/ml murine IFNγ and stimulated with 2 μg/ml LPS. After 24 h, supernatants were collected for analysis of cytokine levels using multiplex ELISAs (mouse pro-inflammatory 7-Plex tissue culture kit measuring IFNγ, IL-1β, IL-10, IL-12p70, IL-6, mKC, TNFα) according to the manufacturer's instructions (Meso Scale Discovery). Cells were lysed in RIPA buffer (25 mM Tris–HCl pH 7.6, 150 mM NaCl, 1% NP-40, 1% sodium deoxycholate, 0.1% sodium dodecyl sulphate (SDS)) for protein measurement by BCA assay (Thermo Scientific).

Cytokine profiling of YAC128 mice

Peritoneal macrophage isolated from wild-type and YAC128 mice were seeded in 24-well plates at a density of 500,000 cells per well. Bone marrow-derived macrophages were used for stimulation experiments after differentiation in 6-well plates at 3×10^6 cells per well. All cultures were primed with 12.5 ng/ml murine IFNγ and stimulated with 100 ng/ml control standard endotoxin (CSE). After 24 h, supernatants were collected for analysis of IL-6 levels by ELISA according to manufacturer's instructions (e-Bioscience). Cells were lysed in RIPA buffer (25 mM Tris–HCl pH7.6, 150 mM NaCl, 1%NP-40, 1% sodium deoxycholate, 0.1% sodium dodecyl sulphate (SDS)) for protein measurement by BCA assay (Thermo Scientific).

Collection and classification of human samples

All human experiments were performed in accordance with the Declaration of Helsinki and approved by the University College London (UCL)/UCL Hospitals Joint Research Ethics Committee. All subjects provided informed written consent. Blood samples were obtained from control subjects and genetically-diagnosed HD patients. Subjects with inflammatory or infective conditions were excluded.

Isolation of human monocytes and macrophages

$CD14^+$ monocytes were isolated from whole blood, as previously described (Bjorkqvist et al., 2008), and differentiated into macrophages by supplementing the RPMI culture medium containing 10% FBS, 2 mM L-glutamine, 50 U/ml penicillin and 50 μg/ml streptomycin (Invitrogen) with 20 ng/ml GM-CSF for 6 days.

Flow cytometry

Up to 1×10^6 cells per well were transferred into a round bottom 96-well plate and centrifuged at 300 ×*g* for 5 min. If necessary the cells were fixed in 4% paraformaldehyde (in PBS). The cells were then gently resuspended in 50 μl of antibody (Table S1) suitably diluted in FACS buffer (PBS with 1% FBS and 0.02% sodium azide). Cells were stained, in the dark, for at least 30 min on a shaker at 4 °C. Afterwards the cells were washed once in 200 μl FACS buffer (centrifuged at 300 ×*g*, 5 min), resuspended in 200 ml FACS buffer, transferred to FACS tubes and analysed using either a special-order BD Bioscience FACScan cytometer (Cytek) with CellQuest Pro (BD Bioscience) and Rainbow (Cytek) software, or a MACSQuant flow cytometer (Miltenyi Biotech) with MACSQuantify software. Data analysis was performed using FlowJo7.2.5 (Tree Star) software. Non-stained and single-colour stained cell controls were always performed.

Cell function assays

Phagocytosis assay

Macrophages were stimulated with 2 μg/ml LPS in R10 media overnight. One hour before the assay, macrophages were washed three times with PBS and serum-free RPMI-1640 was added to the cells. Carboxylate-modified fluorescent yellow-green latex beads (Sigma Aldrich) were added to the cells at a 10:1 ratio and were incubated at 37 °C for 1 h. Cells were then washed with cold PBS twice and incubated with PBS containing 10 nM EDTA for 10 min on ice before the cells were detached from the culture wells by trituration. The cells were then fixed using 3.7% paraformaldehyde for 20 min at room temperature, following which the cells were washed and stained with macrophage-lineage specific cell surface markers for analysis by flow cytometry.

Cell adhesion assay

Peritoneal macrophages were seeded in 24-well plates and left to adhere to the plastic for 2 h. Adhered cells were removed and counted using a Neubauer counting chamber.

Differentiation assay

$CD11b^+$ cells isolated from bone marrow were differentiated using 20 ng/ml recombinant murine M-CSF. After 4 days, undifferentiated monocytes were washed off before differentiated adhered macrophages were lifted of the plastic and counted using a Neubauer counting chamber.

Migration assay

One hundred thousand macrophages were seeded into 8 μm transwell inserts, which were placed into wells filled with RPMI-1640 media containing 1% FBS, 2 mM L-glutamine, 50 units/ml penicillin and 50 mg/ml streptomycin supplemented with 50 ng/ml CCL2 (MCP-1). The cells were incubated for either 90 min or 16 h, after which the inserts were removed from the wells. Cells on the upper side of the insert membrane were gently removed using cotton buds, whilst the cells on the lower side were fixed in ethanol and stained with 1 mg/ml crystal violet. The fixed, stained cells were counted in multiple fields of view using ImageJ software. Pictures were taken using a light microscope (Nikon Eclipse TS100, Objective 20×) with an attached digital camera (Nikon DS-Fi1) and NIS-Elements F 3.00 software.

TR-FRET

The experiment was performed as previously described (Weiss et al., 2012). In brief, cells were lysed in 100 μl PBS containing 1% Triton X-100 and a protease inhibitor cocktail (Roche) per 1×10^6 cells and 5 μl cell lysate was transferred into low-volume wells of white 384-microtitre plates (Greiner). A total of 1 ml detection buffer (50 mM NaH_2PO_4, 400 mM NaF, 0.1% BSA, and 0.05% Tween, plus antibody mix) was added, with the final antibody amount per well for soluble mHTT detection being 0.25 ng 2B7-Tb plus 20 ng MW1-D2. Plates were rotated at 1000 ×*g* for 30 s and incubated for 1 h. TR-FRET readout was performed with an EnVision 102 Reader (PerkinElmer). After the excitation of the donor fluorophore Tb (CisBio) at 320 nm and a time delay of 100 ms, the resulting Tb and acceptor D2 (CisBio) emission signals were read at 620 nm and 665. Ratios of 665/620 nm signals corresponded to mutant HTT levels. HTT protein levels are shown as a percentage of the signal intensity over lysis buffer background signal after normalisation to total protein levels (4F). All assays were carried out blinded to the subject group.

Statistics

Data were analysed using unpaired two-tailed Student's *t*-tests, unless otherwise stated. All error bars represent standard error of the mean.

Results

Cytokine profiling of myeloid cells in R6/2 mice

To determine whether monocytes from HD mouse models are hyper-reactive like those from HD patient blood (Träger et al., 2014), $CD11b^+$ cells from 12-week old R6/2 mice were isolated using magnetic cell sorting and seeded in culture, then primed with IFNγ and stimulated with LPS for 24 h. Analysis of culture supernatants using a multiplex ELISA platform showed an increase in IL-6 and TNFα levels, but not IL-1β, IL-10 and IL-12, produced by R6/2 compared with wild-type cells (Figs. 1A and S1A). Due to the small volumes of fluid available, yields of $CD11b^+$ cells from murine blood are low. To try to identify an alternative source of myeloid cells, other tissues containing monocyte populations were obtained. This also allowed a wider characterisation of HD myeloid cell function. Spleen and bone marrow myeloid cells were isolated and cultured, then primed with IFNγ and stimulated with LPS for 24 h, as before. Spleen myeloid cells from R6/2 mice produced elevated levels of IL-1β and IL-12 compared with wild-type cells, whilst levels of IL-6, TNFα and IL-10 were unchanged (Figs. 1B and S1B). R6/2 bone marrow myeloid cells showed no differences in cytokine production compared with wild-type cells (Figs. 1C and S1C). Therefore, increased cytokine production by hyper-responsive myeloid cells, as seen in HD patients' monocytes and macrophages, was dependent on the tissue origin of myeloid cells in R6/2 mice.

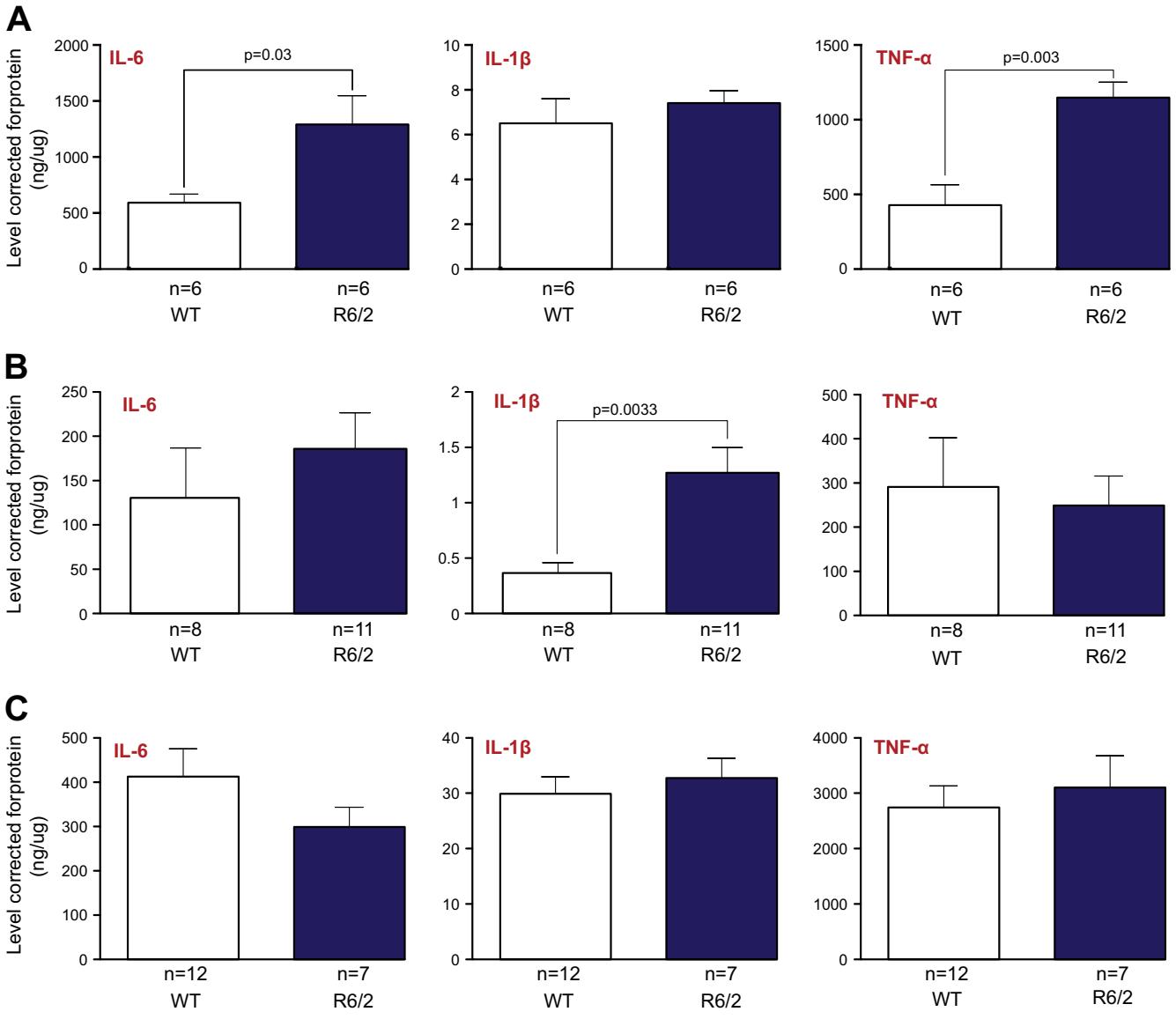

Fig. 1. Altered cytokine production by myeloid cells from R6/2 mice. (A) $CD11b^+$ myeloid cells were isolated from pooled blood samples obtained from 12-week old R6/2 or wild-type mice. Cell cultures primed with IFNγ and stimulated with LPS for 24 h showed significant differences in IL-6 and TNFα production. (B) R6/2 spleen and (C) R6/2 bone marrow myeloid cells were isolated using anti-CD11b magnetic beads, and individual cultures from each mouse were stimulated with IFNγ and LPS for 24 h. Measuring cytokine production in supernatants by multiplex ELISA, R6/2 spleen myeloid cells demonstrated changes in IL-1β levels, whilst bone marrow myeloid cells from R6/2 mice showed the same cytokine levels as wild-type cells. Graphs show mean concentrations corrected to protein content ± SEM. Unpaired two-tailed Student's *t*-tests. (A) n = technical replicates of pooled samples from different mice, (B + C) n = biological replicates representing individual mice.

Cytokine profiling of myeloid cells in full-length HD mouse models

Next, we wanted to see how myeloid cells from mouse models expressing the full-length mHTT protein compared with models such as R6/2 that express an exon 1 fragment of the mutant gene. The knock-in *HdhQ150* model expresses 150 CAG repeats in the endogenous mouse *Htt* gene (Lin et al., 2001). Therefore, we analysed the responsiveness of the myeloid cells from these mice at an age of 22 months (comparable to a R6/2 mouse at 12 weeks).

Cultured *HdhQ150* blood monocytes primed with IFNγ and stimulated with LPS for 24 h demonstrated a significant increase in IL-1β, TNFα and IL-12 production when compared with those from wild-type mice (Figs. 2A and S2A). IL-6 levels were also elevated, but this was not statistically significant (Fig. 2A). Cultured spleen myeloid cells from *HdhQ150* mice stimulated as above demonstrated significantly elevated levels of IL-6 and TNFα, and a slight increase in IL-1β and IL-10, compared with wild-type cells (Figs. 2B and S2B). In contrast, cultured *HdhQ150* bone marrow myeloid cells did not show any differences in cytokine production when stimulated, compared to wild-type cells (Figs. 2C and S2C). This suggests that bone marrow myeloid cells behave differently to other more mature peripheral monocytes and macrophages.

Another full-length mHTT-expressing HD mouse model is the YAC128 model expressing the entire human HD gene (Slow et al., 2003). From this model, bone marrow-derived macrophages from three month old mice were cultured, primed with IFNγ and stimulated with CSE for 24 h. Supernatants from these cultures showed no difference in IL-6 levels when comparing YAC128 and wild-type cells (Fig. 3). This strengthens further the evidence that bone marrow-derived myeloid cells do not show the same mHTT-dependent differences as other, more mature myeloid cell populations, and do not mimic the hyper-responsive phenotype observed in human HD blood-derived monocytes. In contrast, cultured YAC128 peritoneal macrophages stimulated with CSE showed a significant increase in IL-6 production compared with wild-type cells (Fig. 3).

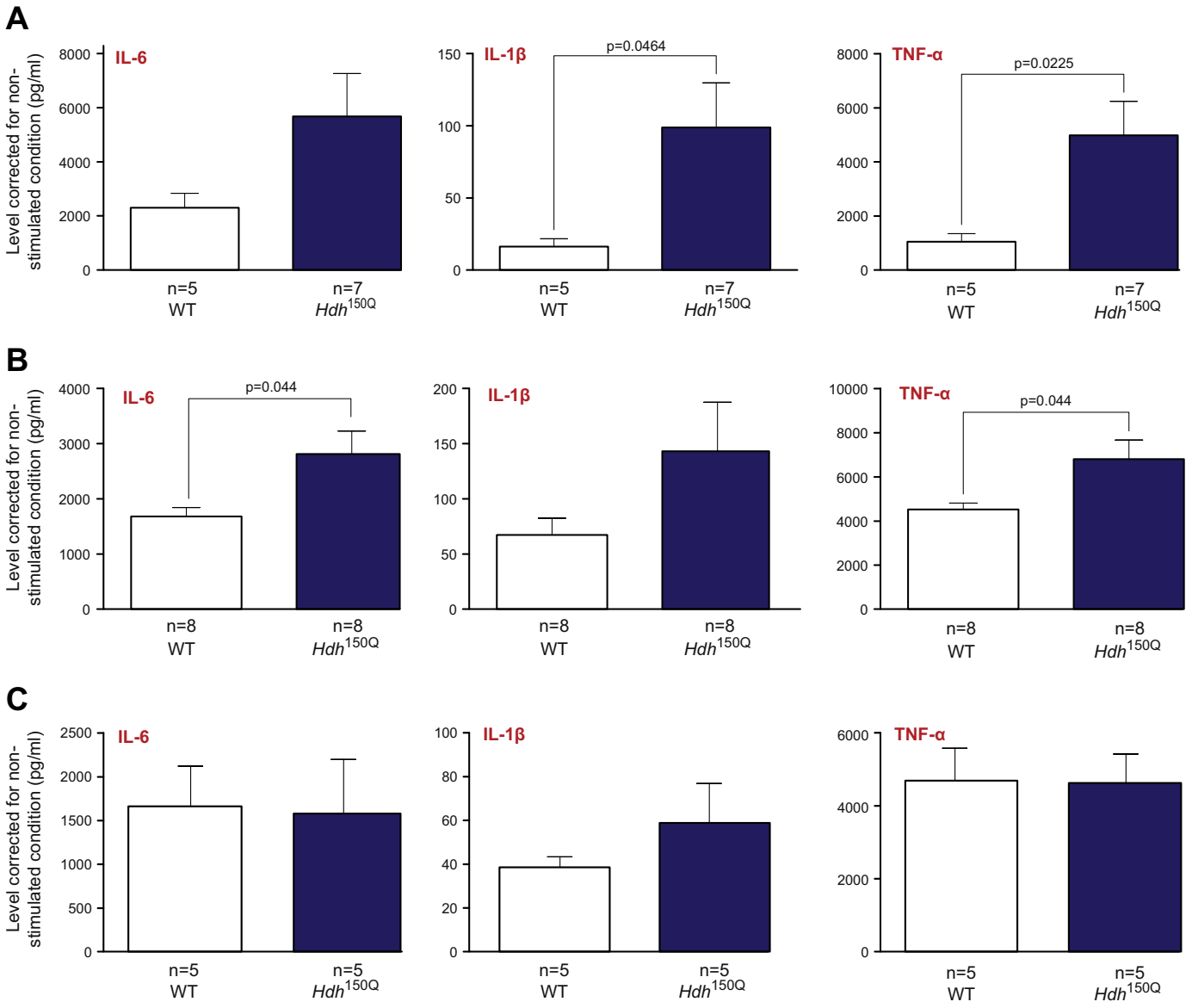

Fig. 2. Altered cytokine production by myeloid cells from *HdhQ150* mice. (A) Blood, (B) spleen and (C) bone marrow myeloid cells were isolated from 22-month old *Hdh*Q150 and wild type mice using anti-CD11b magnetic beads and seeded in culture for stimulation with IFNγ and LPS for 24 h. Cytokine production was analysed by multiplex ELISA. Whilst bone marrow cells produced similar levels of cytokine compared with wild-type, both blood and spleen myeloid cells produced significantly higher levels of pro-inflammatory cytokines. Graphs show mean concentrations corrected to protein content ±SEM. Unpaired two-tailed Student's *t*-tests. n = biological replicates representing individual mice.

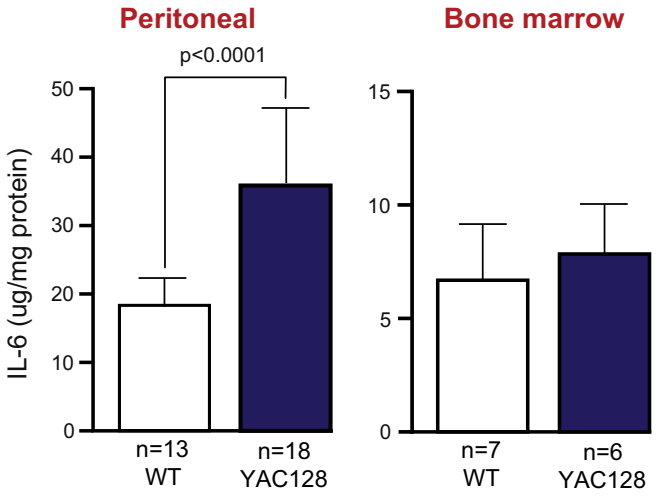

Fig. 3. Altered cytokine production by macrophages from YAC128 mice. Peritoneal macrophages obtained via peritoneal lavage were stimulated with CSE for 24 h before IL-6 levels were measured using ELISA. A significant increase in cytokine production by YAC128 peritoneal macrophages was seen when compared with wild-type. Macrophages were also differentiated from bone marrow monocytes of three month old YAC128 and wild-type mice using M-CSF before stimulation with CSE for 24 h. Measuring IL-6 levels using ELISA showed no difference in cytokine production from YAC128 bone marrow-derived cells compared with wild-type controls. Graphs show mean concentrations corrected to protein content ±SEM. Unpaired two-tailed Student's *t*-tests.

HTT levels in bone marrow and spleen of R6/2 mice

Mutant HTT levels measured in primary human immune cells correlate with markers of disease progression such as disease stage, disease burden score and caudate atrophy (Weiss et al., 2012). Therefore, the observation that mouse myeloid cells isolated from bone marrow appear to be normal compared with more mature myeloid cells isolated from other peripheral tissues may be due to relative differences in the levels of mHTT expression.

However, the measurement of mHTT levels showed that CD11b$^+$ cells isolated from the bone marrow and spleen of 12-week old R6/2 mice are not significantly different (Fig. 4), suggesting that this is not the explanation for why bone marrow myeloid cells from HD mouse models are not hyper-responsive. Interestingly, whilst mHTT levels in whole spleen are similar to those in cells that have been sorted by CD11b$^+$, unsorted bone marrow that contains a large number of stem cells shows increased levels of mHTT expression compared to sorted cells (Fig. 4).

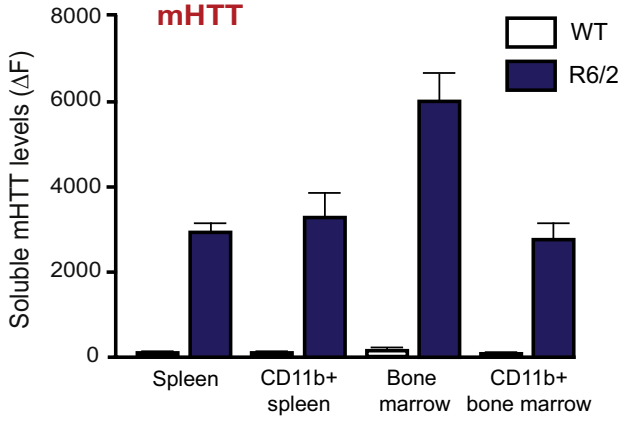

Fig. 4. Mutant HTT levels in R6/2 spleen and bone marrow. Single cell suspensions obtained from bone marrow, spleen as well as magnetically sorted spleen and bone marrow CD11b$^+$ cells from 12-week old R6/2 and wild-type mice (n = 8), were lysed and used to assess mHTT levels. TR-FRET measures demonstrated that mHTT levels are similar in CD11b$^+$ immune cells isolated from spleen and bone morrow. No mHTT was detected in control mice (n = 3). Data shown as percentage of the signal intensities over lysis buffer background signal after normalisation to total protein levels.

CD11b$^+$ cell populations in bone marrow and spleen of R6/2 mice

Differences in cytokine production by myeloid cells from HD and wild-type mice could be accounted for by relative differences in the proportions of different CD11b$^+$ cell populations in the samples. Nearly all cultured CD11b$^+$ cells from blood are monocytes, but in the spleen and bone marrow the CD11b$^+$ population also comprises, for example, macrophages, dendritic cells and granulocytes. To test this in R6/2 mice, CD11b$^+$ cells were isolated from the spleen and bone marrow of transgenic and wild-type mice, as done previously, and stained for flow cytometry quantification of different CD11b$^+$ populations (Fig. S3). In the spleen, most CD11b$^+$ cells were monocytes, macrophages or lymphoid-derived dendritic cells (DCs), whereas in the bone marrow there were many more granulocytes (Table S2). Sorted cells from both tissues contained less than 1.5% contaminating B cells and T cells. There was no evidence of any significant differences between R6/2 and wild-type mice in their spleen and bone marrow CD11b$^+$ populations (Table S2).

R6/2 mouse spleens contain normal proportions of immune cells

We also analysed the proportions of different immune cell subsets within the whole cell population of spleens from 12-week old R6/2 mice. Single cell suspensions prepared from digested spleens were stained with anti-CD3, anti-CD19 and anti-CD11b antibodies as markers for T cells, B cells and myeloid cells, respectively (Fig. 5A). No differences in the proportion of these immune cell populations were found in R6/2 as compared with wild-type spleens (Fig. 5B). Following this, spleen cells were stained with anti-CD3, anti-CD4 and anti-CD8 antibodies to investigate the abundance of CD4$^+$ T_{helper} cells and CD8$^+$ cytotoxic T cells in the spleens of R6/2 mice. However, no differences in T cell subsets were detected in R6/2 spleens when compared with those from wild-type mice (Fig. S4). We also examined myeloid cell subsets, in which spleen cells were stained with anti-F4/80 antibody as a macrophage marker and a combination of anti-CD11c, anti-B220 and anti-CD11b antibodies to distinguish between CD11c$^+$ B220$^+$ plasmacytoid DCs, CD11c$^+$ B220$^-$ CD11b$^-$ lymphoid-derived DCs and CD11c$^+$ B220$^-$ CD11b$^+$ myeloid-derived DCs. Again, no differences in macrophage and DC subsets were detectable in R6/2 compared with wild-type spleens (Fig. S5).

Next, we examined CD11b$^+$ spleen cells more specifically, using MHC class II expression levels to categorise the myeloid cells as being in a resting or activated state (Fig. 6A). Comparing the percentage of resting (CD11b$^+$, MHCII^{low}) and activated (CD11b$^+$, MHCII^{high}) myeloid cells in spleens from 8-week old R6/2 mice did not show a difference between R6/2 and wild-type mice (Fig. 6B), whereas the spleens from 12 week-old animals contained significantly fewer activated myeloid cells and a significantly higher percentage of resting monocytes (Fig. 6C). This may reflect an effect of disease progression as R6/2 mice become symptomatic and closer to end-stage disease at 12 weeks. The altered ratio of resting versus activated myeloid cells may explain the increased IL-1β levels observed in R6/2 spleens.

Functional analysis of monocytes and macrophages in R6/2 mice

Phagocytosis is a key function of macrophages and a significant elevation in phagocytosis was observed in LPS-stimulated blood-derived HD patient macrophages compared with control cells in a flow cytometry based assay (Fig. 7B). To see whether R6/2 mice demonstrate a similar phenotype, bone marrow-derived and peritoneal macrophages were incubated with green fluorescent latex beads and the percentage of cells phagocytosing beads were analysed by flow cytometry. LPS-stimulated bone marrow-derived macrophages from 12-week old R6/2 mice did not demonstrate a difference in phagocytosis levels

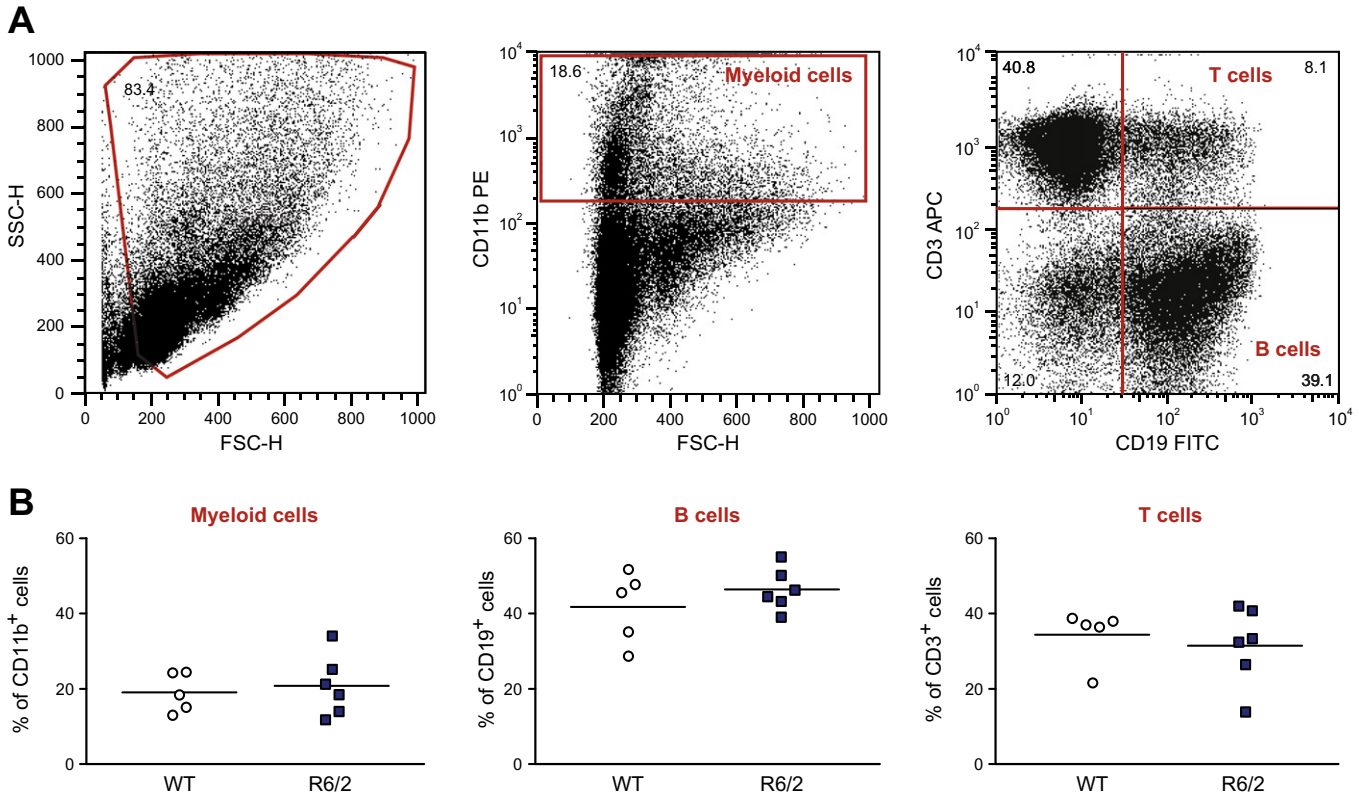

Fig. 5. Splenic B cell, T cell and myeloid cell populations are unchanged in R6/2 mice. (A) Spleens from 12-week old R6/2 and wild-type mice were digested, homogenised and, after red blood cell lysis, stained with anti-CD11b PE, anti-CD3 APC and anti-CD19 FITC antibodies to look for myeloid, T and B cell subsets, respectively. The percentage of each cell population was determined via flow cytometry analysis using the gating as shown. (B) No differences were found comparing R6/2 and wild-type mice spleens using unpaired two-tailed Student's *t*-tests.

compared with wild-type mice (Fig. 7C). Peritoneal macrophages isolated from R6/2 mice, however, showed a small elevation in the percentage of phagocytosing cells upon LPS stimulation, similar to the results in HD patients (Fig. 7D).

Counting the number of differentiated, adhered bone marrow-derived macrophages four days after seeding showed no difference in R6/2 compared with wild-type cells (Fig. 8A). In addition, adhesion of peritoneal macrophages appeared to be normal in R6/2 mice, as the same number of R6/2 and wild-type macrophages adhered to the tissue culture plastic 2 h after seeding (Fig. 8B).

HD patients demonstrate a striking defect in monocyte and macrophage migration towards the chemoattractant MCP-1 in in vitro assays (Kwan et al., 2012b). Furthermore, murine microglia and peritoneal macrophages have been shown to migrate abnormally in vivo (Kwan et al., 2012b). Using the same assay used to assess human HD cells ex vivo, R6/2 mice peritoneal macrophages were seeded on to transwells and the number of cells migrating towards MCP-1 was counted by their location in the lower chamber of the transwell system. Interestingly, peritoneal macrophages from R6/2 and wild-type mice showed similar levels of migration, both under basal conditions and towards MCP-1 after either 90 min or 16 h (Fig. 8C).

Discussion

It has been shown previously that various HD mouse models have increased plasma cytokine levels, including R6/2, *HdhQ150* and YAC128 mouse models (Bjorkqvist et al., 2008). This corresponds to the increased plasma cytokine levels observed in human HD patients (Bjorkqvist et al., 2008). In this study, we show that blood CD11b$^+$ cells isolated from R6/2 and *HdhQ150* are hyper-reactive upon LPS stimulation in vitro, replicating the phenotype observed in human cells. Analysing the cytokine profile in the YAC128 mice, peritoneal macrophages were found to produce high levels of IL-6 upon CSE stimulation. Taken together, all three mouse models recapitulate changed cytokine profiles established in HD patients and therefore they could be used to model the immune phenotype.

However, the origin of the murine myeloid cell is important, demonstrated by a lack of phenotype looking at R6/2, *HdhQ150* and YAC128 bone marrow cells. Neither CD11b$^+$ bone marrow myeloid cells nor macrophages derived from bone marrow cells exhibit increased pro-inflammatory cytokine production or phagocytosis. We did not see a difference in mHTT levels in R6/2 CD11b$^+$ bone marrow compared with mature myeloid cell populations in the spleen, suggesting that mHTT levels are not the reason for the lack of phenotype in the bone marrow. The evidence for a lack of hyper-reactivity in the bone marrow myeloid cells is interesting, particularly in light of a recent paper describing how bone marrow transplants, when given from HD donor to HD recipient mice, can improve certain aspects of HD pathology, such as behavioural changes (Kwan et al., 2012a). Bone marrow transplantation from both wild-type and BACHD mice into irradiated BACHD mice improved the outcome of the balance beam and open field activity task. Whilst it remains to be shown how the transplants confer their benefits, our finding further indicates phenotypic differences between bone marrow and blood myeloid cells that perhaps reflect underlying developmental differences between the two populations.

Looking at cytokine production by CD11b$^+$ myeloid cells isolated from the spleen, *HdhQ150* mice demonstrated elevated IL-6, IL-1β and TNFα levels similar to the changes seen from *HdhQ150* blood monocytes. The same cells from R6/2 mice, however, only showed an increase in IL-1β, whilst IL-6 and TNFα levels were unchanged. In contrast to blood, CD11b$^+$ cells from the spleen comprise a cell suspension that includes macrophages and DCs as well as the desired monocytes. When testing whether a shift in the percentage of these different cell types within the spleen accounts for the rise in IL-1β levels in R6/2 compared

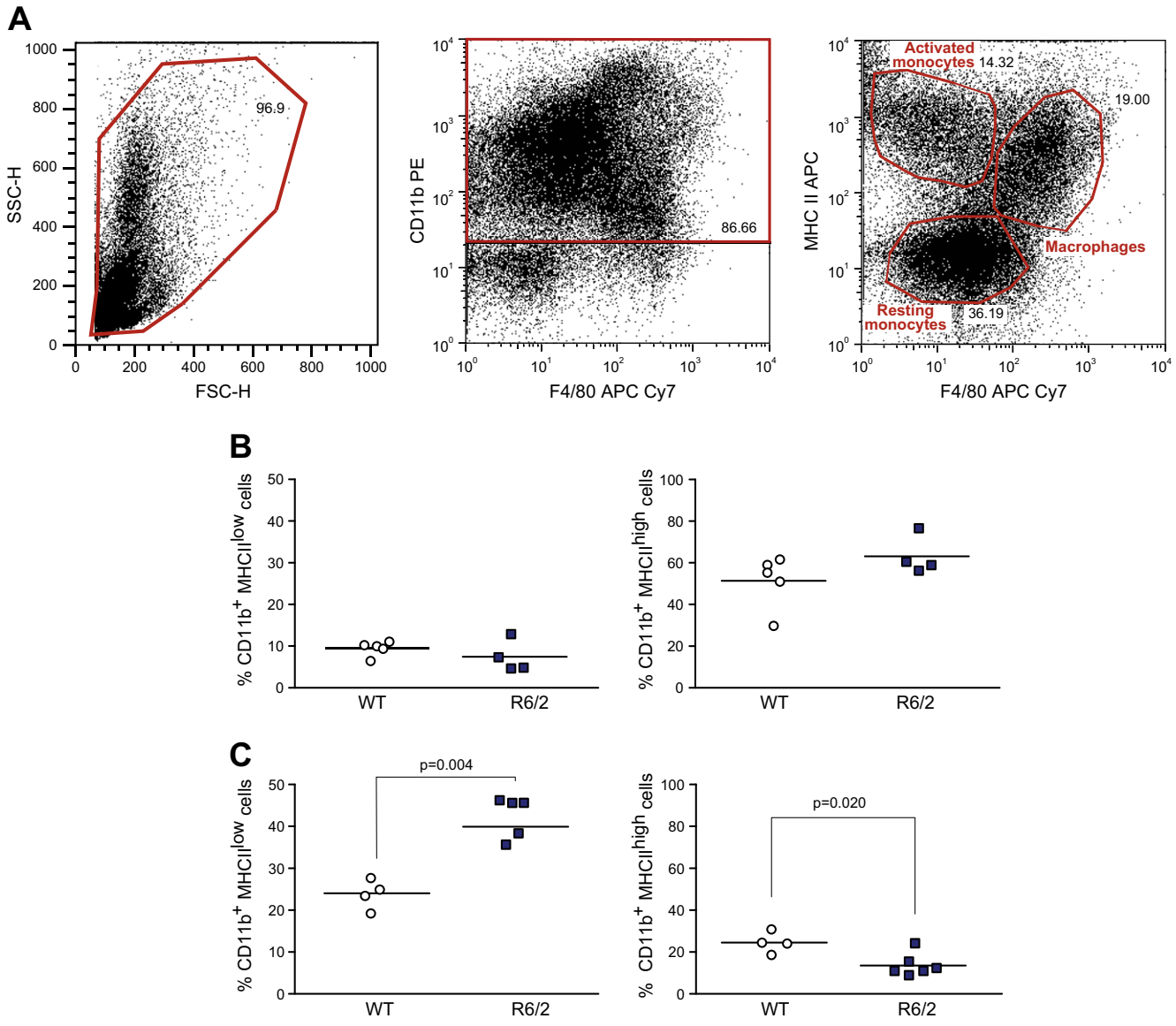

Fig. 6. Ratio of resting versus activated myeloid cells is altered in end-stage R6/2 mice. (A) Spleens were digested, homogenised and, after red blood cell lysis, stained with anti-CD11b PE, anti-CD11c FITC, anti-MHCII APC antibodies. They were analysed by flow cytometry analysis using the gating as shown. (B) At 8 weeks of age, no difference in resting ($CD11b^+$, $MHCII^{low}$) and activated ($CD11b^+$, $MHCII^{high}$) myeloid cells were detected between R6/2 and wild-type mice. (C) At 12 weeks, R6/2 mice demonstrated a significant increase in $CD11b^+/MHCII^{low}$ resting cells whilst $CD11b^+/MHCII^{high}$ activated myeloid cells are significantly decreased. Unpaired two-tailed Student's *t*-test.

with control cells, no differences in the monocyte, macrophage and DC populations were detected. However, when looking at the levels of activation in splenic monocytes using MHC II expression levels as a marker, significantly more resting and fewer activated monocytes were found in R6/2 mice at 12 weeks of age. It might be therefore, that this difference in the isolated population from the spleen and not a cell-intrinsic hyperreactivity of the cells accounts for the difference in IL-1β levels detected in R6/2 spleen. This means that splenic cells from R6/2 mice may not be a good model for the peripheral myeloid cell function in HD.

Looking at other cellular functions, phagocytosis in peritoneal macrophages from R6/2 mice was increased upon LPS stimulation, resembling the human phenotype. However, R6/2 peritoneal macrophages did not demonstrate any migration defect in this study. In a different study, R6/2 mice demonstrate decreased numbers of infiltrating peritoneal macrophages after inducing peritonitis with thioglycolate, when compared with wild-type mice (Kwan et al., 2012b). Although our ex vivo experiments did not show the same trend, it is important to note that the two experiments are not looking at the same aspect of migration. In our in vitro migration assay, the ability of peritoneal macrophages to migrate through a membrane towards one chemokine was tested, whilst an induced peritonitis is not only looking at macrophage migration, but also monocyte infiltration from the blood stream into the peritoneum. This process requires migration through epithelium and cell–cell interactions (Imhof and Aurrand-Lions, 2004), which might be affected in HD and is not modelled in the in vitro assay used here. Furthermore, the in vivo peritonitis experiment showed that R6/2 mice have decreased infiltration of monocytes and macrophages into the peritoneum, but infiltration did still occur (Kwan et al., 2012b). It may be an unintended consequence of isolating a pure population of peritoneal macrophages that more functional cells were isolated, which despite a possible defect managed to migrate into the peritoneum in the first place.

Both fragment R6/2 and full-length (YAC128 and knock-in *HdhQ150*) HD models recapitulate many specific aspects of the human disease, and could be considered for future studies investigating the immune dysfunction in HD and/or targeting it for therapeutics. The use of

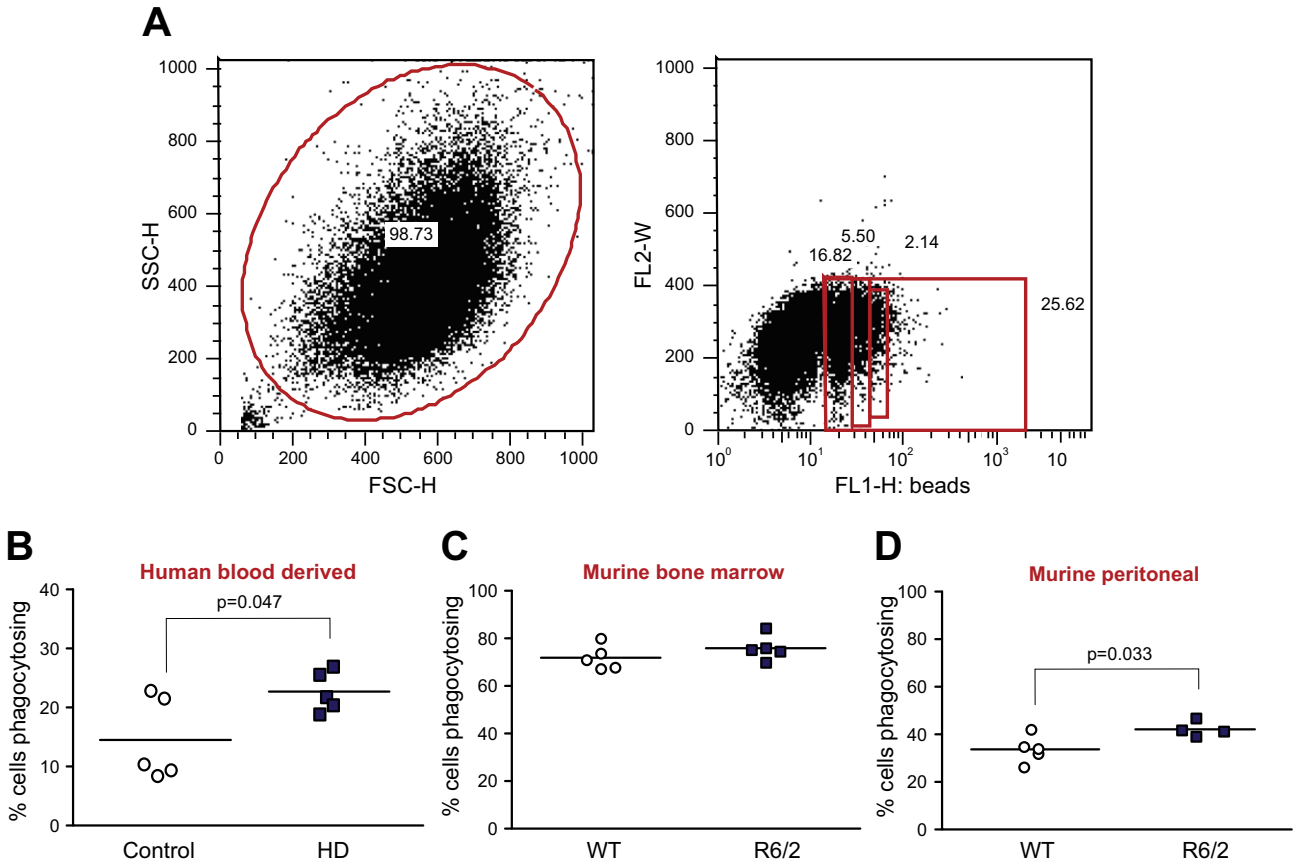

Fig. 7. Phagocytosis levels in macrophages isolated from HD patients and R6/2 mice. (A) Monocyte-derived macrophages were incubated with green fluorescent latex beads for 1 h prior to analysis by flow cytometry of the percentage of cells taking up the beads. Macrophages were gated in the FCS and SSC channels according to their size, and the FL-1 channel was used to determine the percentage of cells that had phagocytosed particular numbers of beads. (B) HD patient macrophages stimulated with LPS for 24 h showed a significant increase in the percentage of phagocytosing cells. n = 5 control and 5 HD patients. (C) Levels of phagocytosis in LPS stimulated bone marrow-derived macrophages were similar in 12-week old wild-type and R6/2 mice, whilst (D) peritoneal macrophages from 12-week old R6/2 mice stimulated with LPS for 24 h showed a significant increase in phagocytosis levels. n = 5 wild-type and n = 4 R6/2 mice. Unpaired two-tailed Student's *t*-test.

mouse models is especially interesting as it allows us to not only study the peripheral immune system, but also the immune cells within the CNS. This will help determine whether peripheral myeloid cells can provide insights into the function of microglia that in humans are inaccessible.

Deciding which tissue is the best for isolation of HD myeloid cells is difficult. Both R6/2 and *HdhQ150* blood monocytes mimic the human monocyte phenotype well and are good models for the human disease, as these are the same cells that the human disease has been studied in. Unfortunately, especially when isolated from 12 week old symptomatic R6/2 mice, only around 100,000 to 300,000 monocytes can be recovered from one mouse. Large animal numbers are therefore required for any experiment. The use of alternative sources for monocytes and macrophages such as bone marrow and spleen demonstrated caveats. The bone marrow myeloid cells and bone marrow-derived macrophages did not show differences in cytokine production and phagocytosis, leading to the conclusion that immature bone marrow cells are not a good model to assess monocyte cell function in HD. Splenic myeloid cells from the R6/2 and *HdhQ150* mouse models, on the other hand, respond in a hyper-reactive manner to LPS, but due to their diverse composition ($CD11b^+$ cells isolated from spleen can be monocytes, macrophages or DCs), this does not resemble studies on human blood cells that are 100% monocytes. As flow cytometry showed that the abundance of the different cell types does not differ between wild-type and R6/2, spleen cells may still be used to compare the genotypes, but conclusions as to which cell type is responsible for differences in phenotype would be difficult to draw.

Having demonstrated the dysfunction of the immune system in HD mouse models in the form of increased plasma cytokine levels (Bjorkqvist et al., 2008) and cytokine production by blood monocytes in vitro, such models can now be used to target molecules in immune pathways that have been identified in human cells. This will further our understanding of the role of the peripheral immune system in HD progression, and help identify and test putative targets for therapeutic intervention.

Acknowledgments

We thank Hayley Lazell, Emma Mead, Julie Moonga and Chris McKinnon for their technical support, members of the Bates group for their breeding and genotyping of the mice, Dr Mark Lowdell for his flow cytometry expertise, and Ray Young for his help with graphics. We also thank the patients and control subjects who donated samples and the staff of the multidisciplinary Huntington's Disease Clinic at the National Hospital for Neurology and Neurosurgery, Queen Square, London.

This study was supported financially by the NIHR University College London Hospitals Biomedical Research Centre (awards to UT and RA (BRC54/NS/RA)), the Medical Research Council (UK) (grant reference no. MR/L02053X/1) and the European Community's Seventh Framework Programme (FP7/2007–2013) (PADDINGTON project; grant agreement no. 261358). SJT also receives support from the CHDI Foundation and the UK Dementia and Neurodegenerative Diseases Network (DeNDRoN).

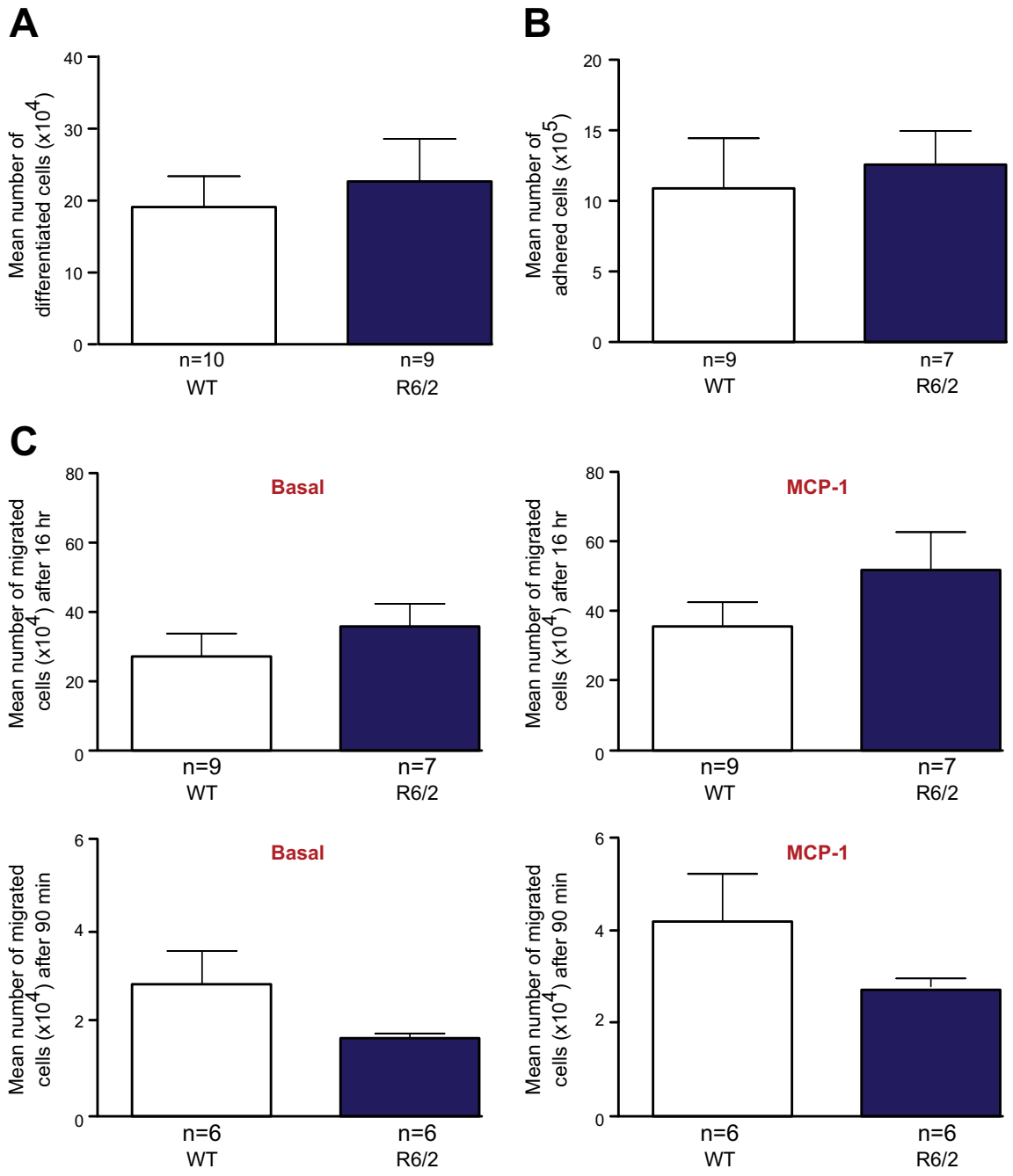

Fig. 8. Myeloid cells from R6/2 mice demonstrate no functional changes in cell adhesion, migration and differentiation. (A) Bone marrow myeloid cells were isolated from 12-week old R6/2 and wild-type mice using anti-CD11b magnetic beads and were differentiated using M-CSF. Four days post seeding, adhered differentiated macrophages were detached and counted. (B) Peritoneal macrophages obtained via peritoneal lavage were seeded onto tissue culture plates. After 2 h the number of adhered cells was counted and no difference in adherence was observed when comparing wild-type and R6/2 cells. Using a transwell system, peritoneal macrophages from R6/2 mice did not show a difference in basal or MCP-1 induced migration after either 16 h or 90 min. Data shown as mean ± SEM. n = biological replicates representing individual mice. Unpaired two-tailed Student's *t*-tests.

Appendix A. Supplementary data

Supplementary data to this article can be found online at http://dx.doi.org/10.1016/j.nbd.2014.10.012.

References

Beck, G., Habicht, G.S., 1996. Immunity and the invertebrates. Sci. Am. 275 (60–3), 66.
Bjorkqvist, M., et al., 2006. Progressive alterations in the hypothalamic–pituitary–adrenal axis in the R6/2 transgenic mouse model of Huntington's disease. Hum. Mol. Genet. 15, 1713–1721.
Bjorkqvist, M., et al., 2008. A novel pathogenic pathway of immune activation detectable before clinical onset in Huntington's disease. J. Exp. Med. 205, 1869–1877.
Crook, Z.R., Houseman, D., 2011. Huntington's disease: can mice lead the way to treatment? Neuron 69, 423–435.
Hockly, E., et al., 2003. Standardization and statistical approaches to therapeutic trials in the R6/2 mouse. Brain Res. Bull. 61, 469–479.
Imhof, B.A., Aurrand-Lions, M., 2004. Adhesion mechanisms regulating the migration of monocytes. Nat. Rev. Immunol. 4, 432–444.
Kazemi-Esfarjani, P., Benzer, S., 2000. Genetic suppression of polyglutamine toxicity in *Drosophila*. Science 287, 1837–1840.
Kuhn, A., et al., 2007. Mutant huntingtin's effects on striatal gene expression in mice recapitulate changes observed in human Huntington's disease brain and do not differ with mutant huntingtin length or wild-type huntingtin dosage. Hum. Mol. Genet. 16, 1845–1861.

Kwan, W., et al., 2012a. Bone marrow transplantation confers modest benefits in mouse models of Huntington's disease. J. Neurosci. 32, 133–142.
Kwan, W., et al., 2012b. Mutant huntingtin impairs immune cell migration in Huntington disease. J. Clin. Invest. 122, 4737–4747.
Labbadia, J., et al., 2011. Altered chromatin architecture underlies progressive impairment of the heat shock response in mouse models of Huntington disease. J. Clin. Invest. 121, 3306–3319.
Li, J.Y., et al., 2005. The use of the R6 transgenic mouse models of Huntington's disease in attempts to develop novel therapeutic strategies. NeuroRx 2, 447–464.
Lin, C.H., et al., 2001. Neurological abnormalities in a knock-in mouse model of Huntington's disease. Hum. Mol. Genet. 10, 137–144.
Mangiarini, L., et al., 1996. Exon 1 of the HD gene with an expanded CAG repeat is sufficient to cause a progressive neurological phenotype in transgenic mice. Cell 87, 493–506.
Moffitt, H., et al., 2009. Formation of polyglutamine inclusions in a wide range of non-CNS tissues in the HdhQ150 knock-in mouse model of Huntington's disease. PLoS ONE 4, e8025.
Parker, J.A., et al., 2001. Expanded polyglutamines in *Caenorhabditis elegans* cause axonal abnormalities and severe dysfunction of PLM mechanosensory neurons without cell death. Proc. Natl. Acad. Sci. U. S. A. 98, 13318–13323.
Sathasivam, K., et al., 2010. Identical oligomeric and fibrillar structures captured from the brains of R6/2 and knock-in mouse models of Huntington's disease. Hum. Med. Genet. 19, 65–78.
Sathasivam, K., et al., 2013. Aberrant splicing of HTT generates the pathogenic exon 1 protein in Huntington disease. Proc. Natl. Acad. Sci. U. S. A. 110, 2366–2370.
Slow, E.J., et al., 2003. Selective striatal neuronal loss in a YAC128 mouse model of Huntington disease. Hum. Mol. Genet. 12, 1555–1567.
The Huntington's Disease Collaborative Research Group, 1993. A novel gene containing a trinucleotide repeat that is expanded and unstable on Huntington's disease chromosomes. The Huntington's Disease Collaborative Research Group. Cell 72, 971–983.
Träger, U., et al., 2014. Immune dysfunction in human HD myeloid cells is caused by NFκB pathway dysregulation and is reversed by lowering HTT levels. Brain 137, 819–833.
van der Burg, J.M., et al., 2009. Beyond the brain: widespread pathology in Huntington's disease. Lancet Neurol. 8, 765–774.
Van Raamsdonk, J.M., et al., 2005. Selective degeneration and nuclear localization of mutant huntingtin in the YAC128 mouse model of Huntington disease. Hum. Mol. Genet. 14, 3823–3835.
Voisine, C., et al., 2007. Identification of potential therapeutic drugs for Huntington's disease using *Caenorhabditis elegans*. PLoS ONE 2, e504.
Vonsattel, J.P., DiFiglia, M., 1998. Huntington disease. J. Neuropathol. Exp. Neurol. 57, 369–384.
Weiss, A., et al., 2012. Mutant huntingtin fragmentation in immune cells tracks Huntington's disease progression. J. Clin. Invest. 122, 3731–3736.
Wild, E., et al., 2011. Abnormal peripheral chemokine profile in Huntington's disease. PLoS Curr. 3 (RRN1231).
Woodman, B., et al., 2007. The Hdh(Q150/Q150) knock-in mouse model of HD and the R6/2 exon 1 model develop comparable and widespread molecular phenotypes. Brain Res. Bull. 72, 83–97.
Yang, S.H., et al., 2008. Towards a transgenic model of Huntington's disease in a non-human primate. Nature 453, 921–924.